JACS
JOURNAL OF THE AMERICAN CHEMICAL SOCIETY
Article
pubs.acs.org/JACS

Toward Organometallic ^{99m}Tc Imaging Agents: Synthesis of Water-Stable ^{99}Tc–NHC Complexes

Michael Benz, Bernhard Spingler, Roger Alberto, and Henrik Braband*

Institute of Inorganic Chemistry, University of Zurich, Winterthurerstrasse 190, 8057 Zurich, Switzerland

Supporting Information

ABSTRACT: $^{99}Tc^{V}O_2$–NHC complexes containing monodentate and bidentate N-heterocyclic carbenes (NHCs) have been prepared by the reactions of $[TcO(glyc)_2]^-$ (glyc = ethyleneglycolato) with 1,3-dimethylimidazoline-2-ylidene (**L1**), 1,1′-methylene-3,3′-dimethyl-4,4′-diimidazoline-2,2′-diylidene (**L2**), and 1,1′-methylene-3,3′-diethyl-4,4′-diimidazoline-2,2′-diylidene (**L3**) in THF. The resulting complexes were fully characterized and their stabilities investigated. While complexes with monodentate NHCs only are hydrolytically unstable, complexes containing bidentate NHCs are water-stable over a broad pH range. The high water stability allows interconversion of the $\{^{99}Tc^{V}O_2\}^+$ core into $\{^{99}Tc^{V}OCl\}^{2+}$ with HCl as the H^+ and Cl^- source. An alternative procedure to obtain $^{99}Tc^{V}O_2$–NHC complexes is the in situ deprotonation of imidazolium salts, enabling the preparation of $^{99}Tc^{V}O_2$–NHC compounds without free NHCs, thus increasing the scope of NHC ligands drastically. The remarkable stability and pH-controllable reactivity of the new complexes underlines the potential of NHCs as stabilizing ligands for ^{99}Tc complexes and paves the way for the first ^{99m}Tc–NHC complexes in the future.

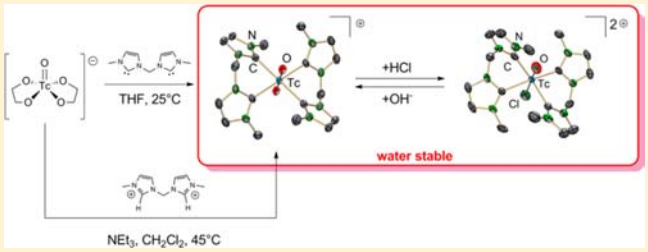

INTRODUCTION

N-Heterocyclic carbenes (NHCs) coordinate to metal centers primarily as strong σ donors, but, depending on the electron configuration at the metal center, act to a lesser degree also as π acceptors.[1,2] This leads to strong ligand–metal bonds that do not easily dissociate.[3,4] These properties render NHCs very versatile ligands, powering strongly increased research activity in organometallic chemistry, particularly in catalysis.[5−9] Besides catalysis, the stability of NHC–metal complexes has encouraged the development of new applications for NHC ligands in other fields such as medicine,[9−15] materials,[10,16] and environmental science.[10,17] For the development of novel classes of technetium-99m (^{99m}Tc) compounds for radiopharmaceutical applications, the use of copper–, silver–, gold–, and palladium–NHC complexes in medicine is particularly interesting. The strong binding of a radiolabel to a targeting vector is a persistent challenge in bioinorganic and radiopharmaceutical drug development. The establishment of NHCs as strongly coordinating ligands in radiopharmacy, in particular in technetium chemistry (over 90% of all diagnostic procedures in nuclear medicine involve ^{99m}Tc-containing compounds),[18] will open additional opportunities for NHC ligands.

Fundamental technetium chemistry is lagging behind that of its heavier congener rhenium. Good examples of these gaps in knowledge are the recent preparations of binary technetium halides such as $TcBr_3$, $TcCl_3$,[19,20] and $TcCl_2$.[21] These fundamental compounds are extremely important, defining general trends in the group 7 transition metals. In this context, the coordination chemistry of NHCs with manganese, technetium, and rhenium has gained much interest over the past years.[22,23] Whereas the number of characterized rhenium complexes is continuously increasing (most of them are low-valent complexes),[22−30] the number of ^{99}Tc complexes is stagnating, likely because of the nucleophilicity of the NHCs.[31−33] Along a triad, redox potentials decrease. Accordingly, rhenium is less oxidizing than its lighter homologues manganese and technetium.[34] It has been demonstrated that Tc^{V} precursors (stable d^2 system) are redox-active, initiated by the strong nucleophilicity of the carbenes. In fact, it is often observed that reaction solutions of Tc^{V} compounds quickly change their color to dark brown after the addition of carbenes, indicating the formation of $Tc^{IV}O_2$, the typical reduction product of higher-valent Tc compounds under basic ambient conditions. Accordingly, the synthesis of ^{99}Tc–NHC complexes has been limited to classes of NHC ligands (i.e., 1,3-dialkyl-4,5-dimethylimidazoline-2-ylidene and 1,2,4-triazolylidene types) that can be prepared without the addition of a strong base such as ^{n}BuLi or KO^{t}Bu.[23,31−33]

Herein we report a general synthetic pathway to $^{99}Tc^{V}O_2$–NHC complexes containing a wide range of NHC ligands, including those derived from imidazolium salts, which have to be generated in situ by the addition of a strong base (Scheme 1). Following this procedure, the first water-stable $^{99}Tc^{V}O_2$–NHC complexes are presented.

Received: September 13, 2013
Published: October 24, 2013

dx.doi.org/10.1021/ja409499u | J. Am. Chem. Soc. 2013, 135, 17566–17572

Scheme 1. General Synthetic Pathway to $^{99}Tc^{V}O_2$–NHC Complexes

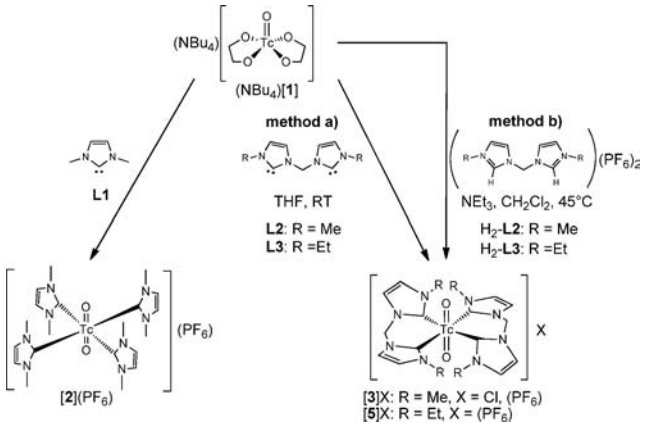

RESULTS AND DISCUSSION

$(NBu_4)[^{99}TcO(glyc)_2]$ ((NBu_4)[**1**]; glyc = ethyleneglycolato) is the starting compound for the newly developed synthetic approach to $^{99}TcO_2$–NHC complexes. (NBu_4)[**1**], first synthesized by Davison et al.,[35] is stable in organic solvents under ambient conditions. Hydrolysis is suppressed by excess ethylene glycol. (NBu_4)[**1**] is prepared from (NBu_4)-$[^{99}TcOCl_4]$ in tetrahydrofuran (THF) according to a procedure described by Braband and Abram[36] and is directly reacted further in situ. Despite its ubiquitous use as a precursor in synthetic ^{99}Tc chemistry, its structure was elusive. We found that upon the addition of Li^+, $[\mathbf{1}]^-$ precipitated from THF as the purple hygroscopic Li[**1**] salt. As a solid, Li[**1**] is stable under dry conditions. It is very soluble in polar organic solvents such as *N*,*N*-dimethylformamide (DMF) and dimethyl sulfoxide (DMSO) but only slightly soluble in THF, MeCN, and CH_2Cl_2. Slow evaporation of a DMF solution of Li[**1**] led to crystals suitable for X-ray diffraction analysis. Figure 1 shows the crystal structure of the $[\mathbf{1}]^-$ anion, which confirms the composition of this intermediate.

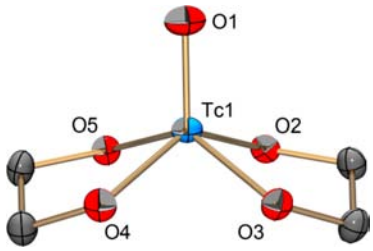

Figure 1. ORTEP representation[37] of the $[^{99}TcO(glyc)_2]^-$ ($[\mathbf{1}]^-$) anion. Thermal ellipsoids represent 50% probability. Hydrogen atoms have been omitted for clarity. Selected bond lengths [Å] and angles [deg]: Tc1–O1 1.660(2), Tc1–O2 1.942(2), Tc1–O3 1.950(2), Tc1–O4 1.949(2), Tc1–O5 1.9383(19); O1–Tc1–O2 111.21(10), O1–Tc1–O3 113.60(10), O1–Tc1–O4 112.11(10), O1–Tc1–O5 110.23(10), O2–Tc1–O3 82.75(10), O4–Tc1–O3 80.86(9).

NHCs such as 1,3-dimethylimidazoline-2-ylidene (**L1**), 1,1′-methylene-3,3′-dimethyl-4,4′-diimidazoline-2,2′-diylidene (**L2**), and 1,1′-methylene-3,3′-diethyl-4,4′-diimidazoline-2,2′-diylidene (**L3**) have to be prepared by deprotonation of the imidazolium salts with ^{n}BuLi or KO^{t}Bu. Upon slow addition of these NHCs to $[\mathbf{1}]^-$ in THF, the corresponding $^{99}Tc^{V}O_2$ complexes $[^{99}TcO_2(\mathbf{L1})_4]^+$ and $[^{99}TcO_2(\mathbf{L2}/\mathbf{L3})_2]^+$, respectively, were formed (Scheme 1). The progress of the reactions was indicated by a color change (purple to yellow). No reductive side reactions were observed.

$[^{99}TcO_2(\mathbf{L1})_4]^+$ ($[\mathbf{2}]^+$) was isolated as orange crystals of $[\mathbf{2}](PF_6)$ from a concentrated reaction solution at −10 °C (55% yield). Figure 2 shows the molecular structure of the

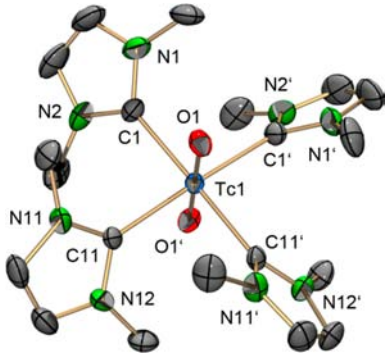

Figure 2. ORTEP representation[37] of the $[^{99}TcO_2(\mathbf{L1})_4]^+$ ($[\mathbf{2}]^+$) cation. Thermal ellipsoids represent 50% probability. Hydrogen atoms have been omitted for clarity. Selected bond lengths [Å] and angles [deg]: Tc1–O1 1.759(2), Tc1–C1 2.191(3), Tc1–C11 2.188(3); O1–Tc1–O1 179.68(15), C11–Tc1–C1′ 177.39(12), O1–Tc1–C1 90.86(12), O1–Tc1–C11 89.03(12), C11–Tc1–C1 90.30(13).

cation $[\mathbf{2}]^+$. $[\mathbf{2}](PF_6)$ crystallizes as $[\mathbf{2}](PF_6)\cdot H_2$-glyc ($H_2$-glyc = ethylene glycol) in the monoclinic space group *C*2/*c*. The ^{99}Tc center is coordinated by four NHC ligands in a paddlewheel-like arrangement, as was found previously for the comparable complex $[^{99}TcO_2(L^{IPr})_4][^{99}TcO_4]\cdot 2.5THF$ (L^{IPr} = 1,3-diisopropyl-4,5-dimethylimidazoline-2-ylidene).[31] The ^{99}Tc–C bond lengths in $[\mathbf{2}](PF_6)\cdot H_2$-glyc, 2.191(3) Å (Tc1–C1) and 2.188(3) Å (Tc1–C11), are slightly shorter than those in $[^{99}TcO_2(L^{IPr})_4][^{99}TcO_4]\cdot 2.5THF$ [2.220(3) – 2.232(3) Å] because of the reduced steric repulsion of ligand **L1** in comparison to L^{IPr}. This becomes clear by comparison with the rhenium complex $[ReO_2(L^{Me})_4](PF_6)_{0.55}[ReO_4]_{0.45}\cdot 2H_2O$ (L^{Me} = 1,3-dimethyl-4,5-dimethylimidazol-2-ylidene), where the Re–C bond lengths [2.19(1) – 2.21(1) Å] are in the exact same range as in $[\mathbf{2}](PF_6)\cdot H_2$-glyc.[38] The Tc1–O1 bond length in $[\mathbf{2}](PF_6)\cdot H_2$-glyc [1.759(2) Å] is similar to the Tc–O bond lengths in $[^{99}TcO_2(L^{IPr})_4][^{99}TcO_4]\cdot 2.5THF$ [1.760(3) and 1.765(2) Å] and $[ReO_2(L^{Me})_4](PF_6)_{0.55}[ReO_4]_{0.45}\cdot 2H_2O$ [1.773(7) and 1.768(7) Å], respectively.

The ^1H NMR spectrum of compound $[\mathbf{2}](PF_6)$ (Figure SI2.2.1 in the Supporting Information) shows only one signal for all of the imidazoline-2-ylidene protons as well as for the protons of the methyl groups. The chemical equivalency of these groups can be rationalized by the symmetry of the *trans*-dioxo complex. Because of scalar coupling to the ^{99}Tc quadrupole nucleus (spin = $^9/_2$), an unambiguous assignment of the weak and broad carbene carbon signals in the ^{13}C NMR spectrum (Figure SI2.2.2) was not possible. The IR spectrum shows the dioxo band ($\nu_{O=Tc=O}$) of $[\mathbf{2}]^+$ at 780 cm^{-1}, which is in the same range as for $[^{99}TcO_2(L^{IPr})_4]^+$ (783 cm^{-1}). In comparison, the $\nu_{O=Re=O}$ band of $[ReO_2(L^{Me})_4]^+$ is found at 768 cm^{-1}.

$[\mathbf{2}](PF_6)$ is stable in the solid state (yellow powder) under an inert atmosphere, but it quickly decomposes in the presence of H_2O and oxygen. These chemical properties are consistent

dx.doi.org/10.1021/ja409499u | J. Am. Chem. Soc. 2013, 135, 17566–17572

with those of other reported $^{99}Tc^{V}$ complexes containing monodentate NHC ligands.[31−33,38] The limited stability renders complexes with the $\{^{99}Tc^{V}O_2\}^+$ core and monodentate NHC ligands not very promising for the further development of imaging agents. Extending the system to bidentate NHC ligands changes the situation substantially, and water-stable $^{99}Tc^{V}O_2$−NHC complexes become accessible.

Starting from the imidazolium salt $(H_2\text{-}\mathbf{L2})(PF_6)_2$, complex $[\mathbf{3}]^+$ was isolated as the salt [**3**]Cl (29% yield) or $[\mathbf{3}](PF_6)$ (50% yield), depending on the synthetic procedure (method a or b, respectively, in Scheme 1). In contrast to all $^{99}Tc^{V}O_2$ compounds with monodentate NHC ligands, $[\mathbf{3}]^+$ is inert against hydrolysis over days at pH ≥7 and up to 50 °C. This remarkable stability of $[\mathbf{3}]^+$ toward hydrolysis and oxidation allowed crystallization directly from H_2O ([**3**]Cl) or a 1:1 H_2O/acetone mixture ($[\mathbf{3}](PF_6)$). Figure 3 shows the molecular structure of the cation $[\mathbf{3}]^+$.

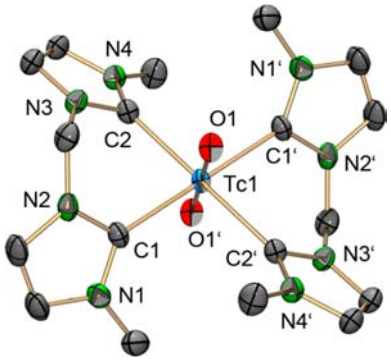

Figure 3. ORTEP representation[37] of the $[^{99}TcO_2(\mathbf{L2})_2]^+$ ($[\mathbf{3}]^+$) cation of the $[\mathbf{3}](PF_6)\cdot H_2O$ structure. Thermal ellipsoids represent 50% probability. Hydrogen atoms have been omitted for clarity. Selected bond lengths [Å] and angles [deg]: Tc1−O1 1.765(3), Tc1−C1 2.170(4), Tc1−C2 2.166(4); O1−Tc−O1′ 180.00(9), O1−Tc1−C1 89.27(15), O1−Tc1−C2 89.24(15), C2−Tc1−C1 81.33(16).

$[\mathbf{3}](PF_6)\cdot H_2O$ crystallizes in the monoclinic space group *P*2/*c*. The conformation of the ligand **L2** inhibits a paddlewheel-like arrangement as in $[\mathbf{2}](PF_6)\cdot H_2$-glyc, and thus, the bidentate ligands coordinate in a more planar fashion. This conformation is a characteristic coordination motif for CH_2-bridged bidentate carbene ligands.[39,40] The Tc−C bond lengths in $[\mathbf{3}](PF_6)\cdot H_2O$, 2.170(4) Å (Tc1−C1) and 2.169(4) Å (Tc1−C2), are significantly shorter than those in $[\mathbf{2}](PF_6)\cdot H_2$-glyc [2.191(3) and 2.188(3) Å], which suggests stronger binding. The ^{1}H NMR spectrum of $[\mathbf{3}](PF_6)$ confirms the high symmetry of the compound (Figure SI2.3.1). Only the signals of the methylene-bridge protons split into doublets, which can be rationalized in terms of the different chemical environments of these two protons (pointing toward and away from the oxo ligand).[40] In comparison to $[\mathbf{2}](PF_6)$ (780 cm^{-1}), the $\nu_{O=Tc=O}$ band of $[\mathbf{3}](PF_6)$ is shifted to lower wavenumber (765 cm^{-1}), which is assumed to be a consequence of the stronger binding of the NHC ligand.

At low pH, compound $[\mathbf{3}]^+$ discloses a unique reactivity: at pH 1, one oxo ligand is reversibly replaced by a chloride to give $[\mathbf{4}]^{2+}$ (Scheme 2). This reactivity is remarkable since the $\{^{99}Tc^{V}O_2\}^+$ core is the thermodynamically most stable metal core for $^{99}Tc^{V}$ and Re^{V} complexes containing NHC ligands under ambient conditions.[23,38] Therefore, this exchange reaction represents the first reversible pH-controlled metal-

Scheme 2. pH-Controlled Ligand Exchange Reactions

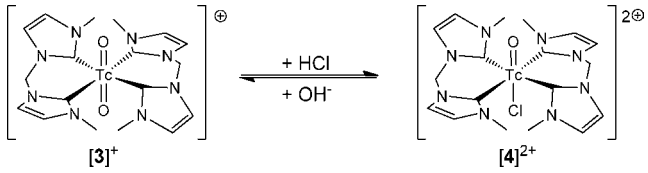

core transformation of an NHC-containing Tc complex (monooxo−dioxo interconversion) without involvement of the equatorial ligands. NMR studies in DMSO-d_6 confirmed the almost quantitative conversion of $[\mathbf{4}]^{2+}$ into $[\mathbf{3}]^+$ after addition of 6 equiv of NaOH (Figure SI2.6). When the "pH" of the DMSO-d_6 solution was decreased by the addition of HCl, $[\mathbf{3}]^+$ was again converted into $[\mathbf{4}]^{2+}$ without decomposition (no increase in the ^{99}Tc NMR signal of $[^{99}TcO_4]^-$). At neutral or acidic pH the NMR probe of $[\mathbf{4}]^{2+}$ did not show any hydrolysis or formation of the dioxo complex $[\mathbf{3}]^+$ (checked over 2 weeks).

Complex $[\mathbf{4}]^{2+}$ was isolated as green crystals of the $(PF_6)^-$ salt from an acidified (1 M HCl, pH 1) 1:1 acetone/H_2O mixture. Whereas the yield in solution was close to quantitative, $[\mathbf{4}](PF_6)_2$ was isolated as a solid in a yield of only 17% because of the increased solubility of $[\mathbf{4}](PF_6)_2$ in H_2O compared with all other $^{99}Tc^{V}O_2$−NHC complexes. $[\mathbf{4}](PF_6)_2$ crystallizes in the triclinic space group *P*1 with two independent cations per asymmetric unit. Both cations disclose a systematic disorder of the O, ^{99}Tc, and Cl atoms along the tetragonal axis (occupancies: Tc1 70:30; Tc2 80:20). The ratios that are both off from 1:1 are the reason why the otherwise existing center of inversion is not present for the whole structure. Figure 4 shows an ORTEP representation[37] of the major species of one cation. Additional information and all of the bond lengths and angles can be found in the Supporting Information.

The IR spectrum of the $[\mathbf{4}](PF_6)_2$ crystals revealed a band at 985 cm^{-1}, which is in the same region as for the comparable Re complex $[ReOCl(L^{Et})_4]^{2+}$ (993 cm^{-1}, L^{Et} = 1,3-diethyl-4,5-dimethylimidazol-2-ylidene).[38] ^{1}H NMR spectroscopy showed four singlets for the backbone imidazoline-2-ylidene protons, four doublets for the CH_2 bridge, and two singlets for the CH_3

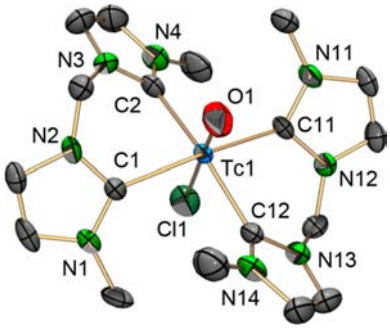

Figure 4. ORTEP representation[37] of the major species of the $[^{99}TcOCl(\mathbf{L2})_2]^{2+}$ ($[\mathbf{4}]^{2+}$) cation in the $[\mathbf{4}](PF_6)_2$ structure. Thermal ellipsoids represent 50% probability. Hydrogen atoms have been omitted for clarity. Selected bond lengths [Å] and angles [deg]: Tc1−O1 1.606(3), Tc1−Cl1 2.4103(15), Tc1−C1 2.155(4), Tc1−C2 2.201(5), Tc1−C11 2.159(4), Tc1−C12 2.131(5); O1−Tc1−Cl1 178.52(12), O1−Tc1−C1 102.66(16), O1−Tc1−C2 99.74(17), O1−Tc1−C11 94.43(15), O1−Tc1−C12 97.16(18), C1−Tc1−C2 81.04(17), C11−Tc1−C12 82.91(17).

dx.doi.org/10.1021/ja409499u | J. Am. Chem. Soc. 2013, 135, 17566−17572

groups (Figure SI2.4.1). This ^{1}H NMR spectrum can be rationalized by the decrease in symmetry caused by the O^{2-}/Cl^{-} ligand exchange. The ^{13}C NMR spectrum is in agreement with these observations: four signals for the backbone imidazoline-2-ylidene carbons, two signals for the CH_2 groups, and two signals for the CH_3 groups (Figure SI2.4.2).

NHCs of the 1,1′-methylene-3,3′-dialkyl-4,4′-diimidazoline-2,2′-diylidene type are highly versatile and can be efficiently modified by altering the alkyl substituents on the nitrogen atoms to optimize the physicochemical properties of the complex. This is demonstrated by the synthesis of compound $[\mathbf{5}]^{+}$, in which the methyl substituents of ligand **L2** have been exchanged for ethyl groups in ligand **L3**. $[\mathbf{5}](PF_6)$ was synthesized by the same procedures as for $[\mathbf{3}](X)$ (X = Cl, PF_6). Figure 5 shows an ORTEP representation[37] of the molecular structure of the $[\mathbf{5}]^{+}$ cation.

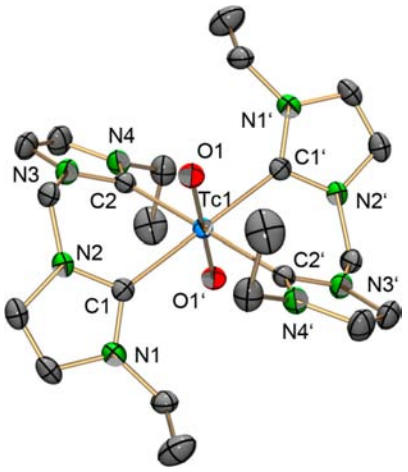

Figure 5. ORTEP representation[37] of the $[^{99}TcO_2(\mathbf{L3})_2]^{+}$ ($[\mathbf{5}]^{+}$) cation of the $[\mathbf{5}](PF_6)\cdot 2.6H_2O$ structure. Thermal ellipsoids represent 50% probability. Hydrogen atoms have been omitted for clarity. Selected bond lengths [Å] and angles [deg]: Tc1−O1 1.762(2), Tc1−C1 2.159(3), Tc1−C2 2.181(3); O1−Tc1−O1′ 180.0, O1−Tc1−C1 90.57(11), O1−Tc1−C2 90.51(11), C1−Tc1−C2 80.47(12).

$[\mathbf{5}](PF_6)$ crystallizes as $[\mathbf{5}](PF_6)\cdot 2.6H_2O$ in the triclinic space group $P\bar{1}$. The asymmetric unit contains two independent ^{99}Tc cations. Since the structural features of the two molecules are very similar (except for disorder at one ethyl group in the Tc2 moiety), only one molecular structure will be discussed (additional structural information is provided in the Supporting Information). The Tc−C bond lengths in $[\mathbf{5}](PF_6)\cdot 2.6H_2O$ [2.159(3) and 2.181(3) Å] differ slightly from the observed bond lengths in $[\mathbf{3}](PF_6)\cdot H_2O$ [2.170(4) and 2.169(4) Å]. Whereas in $[\mathbf{3}](PF_6)\cdot H_2O$ the bond lengths are very similar, in $[\mathbf{5}](PF_6)\cdot 2.6H_2O$ a shortening (Tc1−C1) and elongation (Tc1−C2) of the bonds can be observed. Furthermore, the bite angle of ligand **L3** in $[\mathbf{5}](PF_6)\cdot 2.6H_2O$ [80.47(12)°] is slightly decreased in comparison with that of ligand **L2** in $[\mathbf{3}](PF_6)\cdot H_2O$ [81.33(16)°]. The decrease in the bite angle can be explained by the steric repulsion of the larger ethyl substituents.

The ^{1}H NMR spectrum of complex $[\mathbf{5}]^{+}$ shows the expected set of signals, but they are shifted to higher field compared with those of complex $[\mathbf{3}]^{+}$ (Figure SI2.5.1). The introduction of ethyl groups as substituents on the nitrogen atoms leads to different chemical environments for the backbone imidazoline-2-ylidene carbon atoms. Consequently, these atoms show two signals in the ^{13}C NMR spectrum (121.92 and 119.42 ppm), in contrast to complex $[\mathbf{3}]^{+}$. In the IR spectrum of complex $[\mathbf{5}]^{+}$, the $\nu_{O=Tc=O}$ band can be found at 765 cm^{-1} (the same as for $[\mathbf{3}]^{+}$). Like $[\mathbf{3}]^{+}$, complex $[\mathbf{5}]^{+}$ is stable in aqueous solutions. No decomposition was observed during crystallization from a 1:1 acetone/H_2O solution.

In addition to the presented "classical" two-step procedure for the synthesis of complexes $[\mathbf{2}]^{+}$, $[\mathbf{3}]^{+}$, and $[\mathbf{5}]^{+}$ (generation of the carbene by deprotonation of the imidazolium salt with a strong base, followed by complex formation; Scheme 1, method a), a novel one-step reaction was developed for the synthesis of $[\mathbf{3}]^{+}$ and $[\mathbf{5}]^{+}$ (Scheme 1, method b). This practical synthetic procedure is enabled by the chemical properties of the starting complex $[\mathbf{1}]^{-}$ and the high stability of the target complexes $[\mathbf{3}]^{+}$ and $[\mathbf{5}]^{+}$. In this procedure, the imidazolium salt ($(H_2$-**L2**$)(PF_6)_2$ or $(H_2$-**L3**$)(PF_6)_2$) is suspended in a solution of $[\mathbf{1}]^{-}$ in CH_2Cl_2. The reaction mixture is refluxed for several hours in the presence of excess NEt_3, leading to the formation of $[\mathbf{3}](PF_6)$ or $[\mathbf{5}](PF_6)$, respectively (Scheme 1). This "one-pot" synthesis of ^{99}Tc−NHC complexes has been proven to be an excellent alternative to procedures in which the NHCs are prepared in advance by deprotonation of an imidazolium salt with a strong base. The mild reaction conditions of the reported one-step synthesis also help to control reactions with highly reactive NHC ligands. Therefore, it can be expected that the number of characterized ^{99}Tc−NHC complexes will significantly increase in the future.

■ CONCLUSION

N-Heterocyclic carbenes (NHCs) are ligand systems with prominent potential for a wide range of applications. Recently, their use in life science has drawn enormous attention. To study the application potential of NHC ligands in the field of radiodiagnostics, two synthetic pathways for the synthesis of the first water-stable $^{99}Tc^{V}O_2$−NHC complexes have been developed. As a result of these new synthetic methods, the versatile class of 1,3-dialkylimidazoline-2-ylidene-type NHCs is now available for further studies in the field of technetium chemistry. The isolated water-stable compounds show unique reactivities (pH-controlled metal-core transformation). The presented results are a great step toward the synthesis of water-stable ^{99m}Tc−NHC complexes suitable for radiopharmaceutical applications. Furthermore, they will help to close knowledge gaps in fundamental organometallic technetium chemistry. The possibilities for the development of a synthetic pathway for the synthesis of water-stable $^{99m}Tc^{V}O_2$−NHC complexes are currently being evaluated.

■ EXPERIMENTAL SECTION

Caution: ^{99}Tc is a weak β^{-} emitter. All experiments have to be done in appropriate laboratories approved for handling low-level radioactive materials.

All reactions were carried out under an inert N_2 atmosphere. The imidazolium salt (H-**L1**$)(PF_6)$[41] and the precursor complexes $(NBu_4)[^{99}TcO(glyc)_2]$[42] and $(NBu_4)[^{99}TcOCl_4]$[43] were prepared according to published procedures. The syntheses of the imidazolium salts $(H_2$-**L2**$)(PF_6)_2$[44] and $(H_2$-**L3**$)(PF_6)_2$[45] were adapted from literature procedures and slightly modified (see the Supporting Information). $(NH_4)[^{99}TcO_4]$ (Oak Ridge) and all other chemicals were reagent-grade and used without further purification.

FT-IR spectra were measured on KBr pellets using a PerkinElmer Spectrum Two spectrophotometer. ^{1}H and ^{13}C NMR spectra were recorded on a Bruker DRX500 500 MHz, Bruker AV-400 400 MHz,

dx.doi.org/10.1021/ja409499u | J. Am. Chem. Soc. 2013, 135, 17566−17572

Varian Gemini 300 MHz, or Varian Mercury 200 MHz spectrometer. ^{13}C NMR spectra were proton-decoupled. For technetium content measurements, pure compounds were dissolved in the appropriate solvents. The measurements were carried out with a scintillation cocktail (Packard Ultimate Gold XR) and a liquid scintillation counter (Packard TRICARB 2200CA).

$(NBu_4)[^{99}TcO(glyc)_2]$ ((NBu_4)[1]). $(NBu_4)[^{99}TcOCl_4]$ (24 mg, 0.05 mmol) was dissolved in THF (4 mL), and ethylene glycol (10 μL, 0.18 mmol) was added to the resulting green solution. Dropwise addition of NEt_3 (0.05 mL) led to a color change to purple and the formation of a colorless precipitate, which was filtered off and washed with THF (1 mL). The purple solution of (NBu_4)[**1**] was directly used without further purification. When isolation of Li[**1**] was desired, a suspension of LiCl (2 mg, 0.05 mmol) in THF (1 mL) was added, and the resulting pale-purple solid was filtered off, washed with THF (1 mL), and dried in vacuo. The obtained crude product still contained small amounts of salts such as LiCl and $(NEt_3H)Cl$. Because of the high moisture sensitivity of Li[**1**], no further purification steps were performed. Consequently, no percent yield and technetium content can be given. Yield: 13 mg. ^{1}H NMR (200 MHz, DMF-d_7): δ 4.22−4.00 (m, 8H, CH_2). ^{13}C NMR (75 MHz, DMF-d_7): δ 76.81 (CH_2). Crystals suitable for X-ray diffraction analysis were grown by slow evaporation of a DMF solution.

$[^{99}TcO_2(L1)_4](PF_6)$ ([2](PF_6)). (H-**L1**)(PF_6) (61 mg, 0.25 mmol) was suspended in THF (2 mL), and a solution of KO^{t}Bu (29 mg, 0.26 mmol) in THF (2 mL) was added. After 30 min, the resulting orange solution was added dropwise to a purple solution of (NBu_4)[**1**] (0.05 mmol) in THF (5 mL). The obtained yellow solution was stirred at 25 °C for 1 h. The reaction mixture was filtered, and the volume of the filtrate was reduced to 1 mL under reduced pressure. The solution was stored at −10 °C for 1 week, which led to formation of orange crystals suitable for X-ray diffraction analysis. Removal of the supernatant from the crystals and drying of the crystals in vacuo yielded analytically pure [**2**](PF_6). Yield: 20 mg (55%). ^{1}H NMR (500 MHz, DMSO-d_6): δ 7.34 (s, 8H, Im-H), 3.42 (s, 24H, CH_3). ^{13}C NMR (125 MHz, DMSO-d_6): δ 122.68 (Im-C), 36.07 (CH_3). ^{99}Tc analysis: calcd 13.70%; found 13.27%.

$[^{99}TcO_2(L2)_2]$(X) ([3](X), X = Cl, PF_6). *Method a.* $(H_2$-**L2**$)(PF_6)_2$ (49 mg, 0.10 mmol) was suspended in THF (2 mL), and the suspension was cooled to −78 °C. A solution of ^{n}BuLi (2.5 M in hexane, 0.09 mL, 0.22 mmol) was added, and the solution was slowly warmed to 25 °C under stirring for 3 h. The orange solution was added dropwise to a solution of (NBu_4)[**1**] (0.05 mmol), resulting in a color change to yellow and formation of a precipitate. After 19 h, the solution was filtered. The yellow solid was dissolved in DMF (1.5 mL) and filtered. The solvent was evaporated under a gentle stream of N_2, and the yellow residue was dissolved in MeCN (2 mL). Addition of Et_2O (2 mL) and filtration gave [**3**]Cl as a yellow solid, which was washed with Et_2O (2 mL) and dried in vacuo. Crystals suitable for X-ray diffraction analysis were obtained by storage of a DMF solution at −10 °C. Yield: 8 mg (29%). ^{1}H NMR (500 MHz, DMSO-d_6): δ 7.71 (s, 4H, Im-H), 7.43 (s, 4H, Im-H), 6.92 (d, ^2J(HH) = 12.5 Hz, 2H, CH_2), 6.44 (d, ^2J(HH) = 12.5 Hz, 2H, CH_2), 3.68 (s, 12H, CH_3). ^{13}C NMR (125 MHz, DMSO-d_6): δ 121.56 (Im-C), 62.00 (CH_2), 36.16 (CH_3).

Method b. A solution of (NBu_4)[**1**] (0.04 mmol) in THF was evaporated under reduced pressure, and the purple residue was dissolved in CH_2Cl_2 (10 mL). NEt_3 (0.5 mL) and $(H_2$-**L2**$)(PF_6)_2$ (40 mg, 0.09 mmol) were added, and the solution was heated at 45 °C for 3 h and then cooled to 25 °C. The resulting green solution was filtered to give a pale-yellow crude solid and a green filtrate. The solid was dissolved in a 1:1 acetone/H_2O solution (2 mL). Slow evaporation of the acetone resulted in the formation of [**3**](PF_6) as yellow crystals suitable for X-ray diffraction analysis, which were filtered, washed with H_2O (0.5 mL), and dried in vacuo. After concentration of the green filtrate and storage at −10 °C, a second batch of crystalline [**3**](PF_6) was isolated. Yield: 13 mg (50%). ^{99}Tc analysis: calcd 15.31%; found 14.52%. IR (KBr): 847 cm^{-1} (s, $(PF_6)^-$). Other analytical data are in accordance with those of [**3**]Cl.

$[^{99}TcOCl(L2)_2](PF_6)_2$ ([4]$(PF_6)_2$). A solution of (NBu_4)[**1**] (0.1 mmol) in THF was evaporated under reduced pressure, and the purple residue was dissolved in CH_2Cl_2 (10 mL). NEt_3 (0.5 mL) and $(H_2$-**L2**$)(PF_6)_2$ (92 mg, 0.2 mmol) were added, and the solution was heated at 45 °C for 7 h and then cooled to 25 °C. The resulting green solution was filtered to give a pale-yellow crude solid and a green filtrate. The crude solid was washed with CH_2Cl_2 (2 mL) and acetone (2 × 1 mL). The yellow residue was dissolved in a 1:1 acetone/H_2O solution (2 mL). Addition of 1 M HCl (100 μL, pH 1) resulted in a color change to green. Slow evaporation of the acetone yielded [**4**]$(PF_6)_2$ as green crystals suitable for X-ray diffraction analysis, which were filtered, washed with Et_2O (1 mL), and dried in vacuo. Yield (based on (NBu_4)[**1**]): 13 mg (17%). ^{1}H NMR (500 MHz, DMSO-d_6): δ 8.14 (s, 2H, Im-H), 8.09 (s, 2H, Im-H), 8.03 (s, 2H, Im-H), 7.80 (s, 2H, Im-H), 7.05 (d, ^2J(HH) = 14 Hz, 1H, CH_2), 6.92 (dd, ^2J(HH) = 13.5 Hz, 2H, CH_2), 6.54 (d, ^2J(HH) = 14 Hz, 1H, CH_2), 3.88 (s, 6H, CH_3), 3.55 (s, 6H, CH_3). ^{13}C NMR (125 MHz, DMSO-d_6): δ 125.60 (Im-C), 125.22 (Im-C), 125.15 (Im-C), 123.36 (Im-C), 64.16 (CH_2), 62.38 (CH_2), 38.15 (CH_3), 36.81 (CH_3). ^{99}Tc analysis: calcd 12.49%; found 12.29%.

$[^{99}TcO_2(L3)_2](PF_6)$ ([5](PF_6)). *Method a.* $(H_2$-**L3**$)(PF_6)_2$ (50 mg, 0.10 mmol) was suspended in THF (6 mL), and the reaction mixture was cooled to −78 °C. A solution of ^{n}BuLi (1.6 M in hexane, 0.13 mL, 0.21 mmol) was added, and the solution was slowly warmed to 25 °C under stirring for 3 h. The colorless solution was added dropwise to a solution of (NBu_4)[**1**] (0.05 mmol), resulting in a color change to yellow and formation of a precipitate. After 2 h, the suspension was filtered, and the yellow solid was washed with THF (1 mL) and H_2O (1 mL). The crude solid was dissolved in a 1:1 acetone/H_2O solution (2 mL). Slow evaporation of the acetone resulted in formation of [**5**](PF_6) as yellow crystals that were analyzed by X-ray diffraction. The crystals were filtered, washed with H_2O (1 mL) and $CHCl_3$ (1 mL), and dried in vacuo. Yield: 12 mg (33%). ^{1}H NMR (400 MHz, MeCN-d_3): δ 7.55 (s, 4H, Im-H), 7.30 (s, 4H, Im-H), 7.15 (d, ^2J(HH) = 12.4 Hz, 2H, $CH_{2\ bridge}$), 6.14 (d, ^2J(HH) = 12.4 Hz, 2H, $CH_{2\ bridge}$), 4.29−4.09 (m, 8H, CH_3CH_2N), 1.21 (t, ^3J(HH), 7.2 Hz, 12H, CH_3CH_2N). ^{13}C NMR (100 MHz, MeCN-d_3): δ 121.92 (Im-C), 119.42 (Im-C), 62.78 ($CH_{2\ bridge}$), 44.77 (CH_3CH_2N), 15.07 (CH_3CH_2N). ^{99}Tc analysis: calcd 13.54%; found 12.60%.

Method b. A solution of (NBu_4)[**1**] (0.10 mmol) in THF was evaporated under reduced pressure, and the purple residue was dissolved in CH_2Cl_2 (5 mL). NEt_3 (1 mL) and $(H_2$-**L3**$)(PF_6)_2$ (97 mg, 0.20 mmol) were added, and the solution was heated at 45 °C for 3 h and then cooled to 25 °C. The resulting green solution was filtered to give a pale-yellow crude solid and a green filtrate. The crude solid was washed with cold MeCN (3 × 0.5 mL), and the obtained yellow solid was dried in vacuo. Yield: 18 mg (26%). ^{99}Tc analysis: calcd 14.46%; found 13.19%. Other analytical data are in accordance with those for the product obtained using method a.

X-ray Diffraction. Crystallographic data were collected at 183(2) K with Mo Kα radiation (λ = 0.7107 Å) that was monochromatized with the help of graphite on either a Stoe IPDS 2T diffractometer (Li[**1**]·DMF, [**3**]Cl·H_2O, [**3**](PF_6)·H_2O) or an Oxford Diffraction Xcalibur system ([**2**](PF_6)·H_2-glyc, [**4**]$(PF_6)_2$, [**5**](PF_6)·2.6H_2O) with a Ruby detector. Suitable crystals were covered with oil (Infineum V8512, formerly known as Paratone N), mounted on top of a glass fiber, and immediately transferred to the diffractometer. In the case of the IPDS, a maximum of 8000 reflections distributed over the whole limiting sphere were selected by the program SELECT and used for unit cell parameter refinement with the program CELL.[46] Data were corrected for Lorentz and polarization effects as well as for absorption (numerical). In the case of the Oxford system, the CrysAlis^{Pro} program suite was used for data collection, semiempirical absorption correction, and data reduction.[47] More details on data collection and structure calculations are contained in Table SI1 in the Supporting Information. Structures were solved with direct methods using SIR97[48] and were refined by full-matrix least-squares methods on F^2 with SHELXL-97. The refinements were done with anisotropic thermal parameters for all non-hydrogen atoms, unless otherwise mentioned. The positions of the hydrogen atoms (except hydrogen atoms of water molecules) were

calculated using the "riding model" option of SHELXL97.[49] Hydrogen atoms of water molecules in structures [3]Cl·H_2O, [3](PF_6)·H_2O, and [5](PF_6)·2.6H_2O were assigned from the Fourier map and refined with fixed bond lengths and angles (1,3-atom restraints) (DFIX).

The crystal structure of compound [4](PF_6)$_2$ had to be refined as an inversion twin. Furthermore, some disorders were considered during the refinement of the structure. The crystal structure discloses two independent $[4]^+$ cations and four $(PF_6)^-$ anions. Both cations are systematically disordered along the tetragonal axis (occupancies: Tc1 70:30; Tc2 80:20). This disorder had to be taken into account in determining the space group of compound [4](PF_6)$_2$ ($P1$ not $P\bar{1}$). The Tc atoms are located above and below the plane defined by the carbene carbon atoms [plane$_{C1,C2,C11,C12}$: Tc1a = 0.320(0.003) Å, Tc1b = 0.493(0.003) Å; plane$_{C21,C22,C31,C32}$: Tc2a = 0.344 (0.003) Å, Tc2b = 0.592(0.003) Å]. Because of this disorder, the atoms O1/Cl1b and O1b/Cl1 are located (and were refined) at the same positions. Atoms O2b and Cl2b were refined isotropically.

In the crystal structure of compound [5](PF_6)·2.6H_2O, the water oxygen atom O41 shows an occupancy of 0.6, which was taken into account during the refinement.

Additional information on the structure determinations has been deposited with the Cambridge Crystallographic Data Centre.

■ ASSOCIATED CONTENT

Supporting Information

Ligand and complex synthesis including IR data, NMR data as well as crystallographic details. This material is available free of charge via the Internet at http://pubs.acs.org.

■ AUTHOR INFORMATION

Corresponding Author

Phone: +41 44 63 54611. E-mail: braband@aci.uzh.ch.

Notes

The authors declare no competing financial interest.

■ ACKNOWLEDGMENTS

H.B. and M.B. acknowledge financial support from the Swiss National Science Foundation (PZ00P2_143102 and 200021_140665/1).

■ REFERENCES

(1) Hu, X.; Castro-Rodriguez, I.; Olsen, K.; Meyer, K. *Organometallics* **2004**, *23*, 755−764.
(2) Nemcsok, D.; Wichmann, K.; Frenking, G. *Organometallics* **2004**, *23*, 3640−3646.
(3) Herrmann, W. A.; Goossen, L. J.; Spiegler, M. *Organometallics* **1998**, *17*, 2162−2168.
(4) McGuinness, D. S.; Cavell, K. J.; Skelton, B. W.; White, A. H. *Organometallics* **1999**, *18*, 1596−1605.
(5) Herrmann, W. A. *Angew. Chem., Int. Ed.* **2002**, *41*, 1290−1309.
(6) Bourissou, D.; Guerret, O.; Gabbai, F. P.; Bertrand, G. *Chem. Rev.* **2000**, *100*, 39−92.
(7) Melaimi, M.; Soleilhavoup, M.; Bertrand, G. *Angew. Chem., Int. Ed.* **2010**, *49*, 8810−8849.
(8) Hahn, F. E.; Jahnke, M. C. *Angew. Chem., Int. Ed.* **2008**, *47*, 3122−3172.
(9) César, V.; Gade, L. H.; Bellemin-Laponnaz, S.; Delaude, L.; Demonceau, A.; Krüger, A.; Albrecht, M.; Marion, N.; Normand, A. T.; Cavell, K. J.; Jahnke, M. C.; Hahn, F. E.; Häller, L. J. L.; Macgregor, S. A.; Panetier, J. A.; Praetorius, J. M.; Crudden, C. M.; Chiang, P.-C.; Bode, J. W.; Çetinkaya, B.; Deblock, M. C.; Panzner, M. J.; Tessier, C. A.; Cannon, C. L.; Youngs, W. J.; Schaper, L.-A.; Tosh, E.; Herrmann, W. A.; Podhajsky, S. M.; Sigman, M. S.; Fort, Y.; Com, C. *N-Heterocyclic Carbenes*; RSC Publishing: Cambridge, U.K., 2011; Vol. *6*, p 442.
(10) Mercs, L.; Albrecht, M. *Chem. Soc. Rev.* **2010**, *39*, 1903−1912.
(11) Hindi, K. M.; Panzner, M. J.; Tessier, C. A.; Cannon, C. L.; Youngs, W. J. *Chem. Rev.* **2009**, *109*, 3859−3884.
(12) Garrison, J. C.; Youngs, W. J. *Chem. Rev.* **2005**, *105*, 3978−4008.
(13) Barnard, P. J.; Berners-Price, S. J. *Coord. Chem. Rev.* **2007**, *251*, 1889−1902.
(14) Kascatan-Nebioglu, A.; Panzner, M. J.; Tessier, C. A.; Cannon, C. L.; Youngs, W. J. *Coord. Chem. Rev.* **2007**, *251*, 884−895.
(15) Teyssot, M.-L.; Jarrousse, A.-S.; Manin, M.; Chevry, A.; Roche, S.; Norre, F.; Beaudoin, C.; Morel, L.; Boyer, D.; Mahiou, R.; Gautier, A. *Dalton Trans.* **2009**, 6894−6902.
(16) Chi, Y.; Chou, P.-T. *Chem. Soc. Rev.* **2010**, *39*, 638−655.
(17) Zhang, Y.; Chan, J. Y. G. *Energy Environ. Sci.* **2010**, *3*, 408−417.
(18) Roesch, F.; Knapp, F. F. *Handbook of Nuclear Chemistry*; Kluwer: Dordrecht, The Netherlands, 2003; Vol. *4*, pp 81−118.
(19) Poineau, F.; Johnstone, E. V.; Weck, P. F.; Kim, E.; Forster, P. M.; Scott, B. L.; Sattelberger, A. P.; Czerwinski, K. R. *J. Am. Chem. Soc.* **2010**, *132*, 15864−15865.
(20) Poineau, F.; Rodriguez, E. E.; Forster, P. M.; Sattelberger, A. P.; Cheetham, A. K.; Czerwinski, K. R. *J. Am. Chem. Soc.* **2009**, *131*, 910−911.
(21) Poineau, F.; Malliakas, C. D.; Weck, P. F.; Scott, B. L.; Johnstone, E. V.; Forster, P. M.; Kim, E.; Kanatzidis, M. G.; Czerwinski, K. R.; Sattelberger, A. P. *J. Am. Chem. Soc.* **2011**, *133*, 8814−8817.
(22) Hock, S. J.; Schaper, L.-A.; Herrmann, W. A.; Kuhn, F. E. *Chem. Soc. Rev.* **2013**, *42*, 5073−5089.
(23) Braband, H.; Kückmann, T. I.; Abram, U. *J. Organomet. Chem.* **2005**, *690*, 5421−5429.
(24) Kaufhold, O.; Stasch, A.; Edwards, P. G.; Hahn, F. E. *Chem. Commun.* **2007**, 1822−1824.
(25) Kaufhold, O.; Stasch, A.; Pape, T.; Hepp, A.; Edwards, P. G.; Newman, P. D.; Hahn, F. E. *J. Am. Chem. Soc.* **2009**, *131*, 306−317.
(26) Flores-Figueroa, A.; Kaufhold, O.; Feldmann, K.-O.; Hahn, F. E. *Dalton Trans.* **2009**, 9334−9342.
(27) Huertos, M. A.; Pérez, J.; Riera, L.; Menéndez-Velázquez, A. *J. Am. Chem. Soc.* **2008**, *130*, 13530−13531.
(28) Huertos, M. A.; Pérez, J.; Riera, L.; Díaz, J.; López, R. *Chem.—Eur. J.* **2010**, *16*, 8495−8507.
(29) Huertos, M. A.; Pérez, J.; Riera, L.; Díaz, J.; López, R. *Angew. Chem., Int. Ed.* **2010**, *49*, 6409−6412.
(30) Hiltner, O.; Herdtweck, E.; Drees, M.; Herrmann, W. A.; Kühn, F. E. *Eur. J. Inorg. Chem.* **2009**, 1825−1831.
(31) Braband, H.; Zahn, T. I.; Abram, U. *Inorg. Chem.* **2003**, *42*, 6160−6162.
(32) Braband, H.; Abram, U. *Organometallics* **2005**, *24*, 3362−3364.
(33) Oehlke, E.; Kong, S.; Arciszewski, P.; Wiebalck, S.; Abram, U. *J. Am. Chem. Soc.* **2012**, *134*, 9118−9121.
(34) Abram, U. Rhenium. In *Comprehensive Coordination Chemistry II*; McCleverty, J. A., Meyer, T. J., Eds.; Elsevier Pergamon: Amsterdam, 2003; Vol. *5*, pp 271−402.
(35) Davison, A.; DePamphilis, B. V.; Jones, A. G.; Franklin, K. J.; Lock, C. J. L. *Inorg. Chim. Acta* **1987**, *128*, 161−167.
(36) Braband, H.; Abram, U. *Inorg. Chem.* **2006**, *45*, 6589−6591.
(37) Farrugia, L. J. *ORTEP-3 for Windows: A Version of ORTEP-III with a Graphical User Interface (GUI)*; University of Glasgow: Glasgow, U.K., 1997.
(38) Kückmann, T. I.; Abram, U. *Inorg. Chem.* **2004**, *43*, 7068−7074.
(39) Hahn, F. E.; Foth, M. *J. Organomet. Chem.* **1999**, *585*, 241−245.
(40) Öfele, K.; Herrmann, W. A.; Mihalios, D.; Elison, M.; Herdtweck, E.; Priermeier, T.; Kiprof, P. *J. Organomet. Chem.* **1995**, *498*, 1−14.
(41) Buitrago, E.; Tinnis, F.; Adolfsson, H. *Adv. Synth. Catal.* **2012**, *354*, 217−222.
(42) Braband, H.; Tooyama, Y.; Fox, T.; Alberto, R. *Chem.—Eur. J.* **2009**, *15*, 633−638.
(43) Poineau, F.; Sattelberger, A. P.; Czerwinski, K. R. *J. Coord. Chem.* **2008**, *61*, 2356−2370.
(44) Cao, C.; Zhuang, Y.; Zhao, J.; Liu, H.; Geng, P.; Pang, G.; Shi, Y. *Synth. Commun.* **2012**, *42*, 380−387.

(45) In, S.; Kang, J. *J. Inclusion Phenom. Macrocyclic Chem.* **2006**, *54*, 129−132.
(46) *STOE-IPDS Software Package*; STOE & Cie GmbH: Darmstadt, Germany, 1999.
(47) *CrysAlis^{Pro} Software System*, version 171.32; Oxford Diffraction Ltd.: Oxford, U.K., 2007.
(48) Altomare, A.; Burla, M. C.; Camalli, M.; Cascarano, G. L.; Giacovazzo, C.; Guagliardi, A.; Moliterni, A. G. G.; Polidori, G.; Spagna, R. *J. Appl. Crystallogr.* **1999**, *32*, 115−119.
(49) Sheldrick, G. *Acta Crystallogr., Sect. A* **2008**, *64*, 112−122.